AD-758 774

# DESIGNS AND EXPERIMENTS RELATING TO STABLE GAS LASERS

Charles Freed

Massachusetts Institute of Technology

Prepared for:

Electronic Systems Division
Advanced Research Projects Agency

1 March 1973

ESD-TR-73-65



# Technical Note

1973-14

C. Freed

# Designs and Experiments Relating to Stable Gas Lasers

1 March 1973

Prepared for the Advanced Research Projects Agency
under Electronic Systems Division Contract F19628-73-C-0002 by

**Lincoln Laboratory**

MASSACHUSETTS INSTITUTE OF TECHNOLOGY

LEXINGTON, MASSACHUSETTS

UNCLASSIFIED

Security Classification

## DOCUMENT CONTROL DATA – R&D

*(Security classification of title, body of abstract and indexing annotation must be entered when the overall report is classified)*

| | |
|---|---|
| 1. ORIGINATING ACTIVITY *(Corporate author)*<br>Lincoln Laboratory, M.I.T. | 2a. REPORT SECURITY CLASSIFICATION<br>Unclassified<br>2b. GROUP<br>None |

3. REPORT TITLE

Designs and Experiments Relating to Stable Gas Lasers

4. DESCRIPTIVE NOTES *(Type of report and inclusive dates)*

Technical Note

5. AUTHOR(S) *(Last name, first name, initial)*

Freed, Charles

| | | |
|---|---|---|
| 6. REPORT DATE<br>1 March 1973 | 7a. TOTAL NO. OF PAGES<br>~~38~~ 36 | 7b. NO. OF REFS<br>10 |
| 8a. CONTRACT OR GRANT NO. F19628-73-C-0002<br>b. PROJECT NO. ARPA Order 600<br>c.<br>d. | 9a. ORIGINATOR'S REPORT NUMBER(S)<br>Technical Note 1973-14<br>9b. OTHER REPORT NO(S) *(Any other numbers that may be assigned this report)*<br>ESD-TR-73-65 | |

10. AVAILABILITY/LIMITATION NOTICES

Approved for public release; distribution unlimited.

| | |
|---|---|
| 11. SUPPLEMENTARY NOTES<br>None<br>**Details of illustrations in this document may be better studied on microfiche.** | 12. SPONSORING MILITARY ACTIVITY<br>Advanced Research Projects Agency, Department of Defense |

13. ABSTRACT

This report describes some of the advances in the design and performance of stable gas lasers. The construction and output characteristics of highly reproducible, stable, selectable single transition grating-controlled $CO_2$ and CO lasers are described. Experiments on short-term stability, standing wave saturation resonances, pressure and power broadening, pressure shift and long-term stabilization of $CO_2$ lasers are discussed.

14. KEY WORDS

stable gas lasers
$CO_2$ lasers
optical radar
infrared wavelengths



UNCLASSIFIED

Security Classification

MASSACHUSETTS INSTITUTE OF TECHNOLOGY

LINCOLN LABORATORY

# DESIGNS AND EXPERIMENTS RELATING TO STABLE GAS LASERS

*CHARLES FREED*

*Group 54*

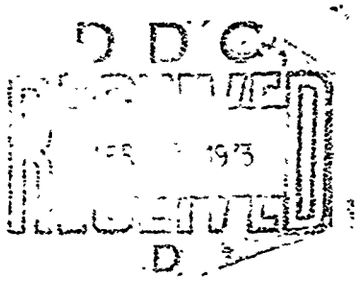


TECHNICAL NOTE 1973-14

1 MARCH 1973



LEXINGTON MASSACHUSETTS

The work reported in this document was performed at Lincoln Laboratory, a center for research operated by Massachusetts Institute of Technology. This work was sponsored by the Advanced Research Projects Agency of the Department of Defense under Air Force Contract F19628-73-C-0002 (ARPA Order 600).

HL

## ABSTRACT

This report describes some of the advances in the design and performance of stable gas lasers. The construction and output characteristics of highly reproducible, stable, selectable single transition grating-controlled $CO_2$ and CO lasers are described. Experiments on short-term stability, standing wave saturation resonances, pressure and power broadening, pressure shift and long-term stabilization of $CO_2$ lasers are discussed.


Accepted for the Air Force
Joseph J. Whelan, USAF
Acting Chief, Lincoln Laboratory Liaison Office

# DESIGNS AND EXPERIMENTS RELATING TO STABLE GAS LASERS

## I. INTRODUCTION

This paper describes some of the advances[1] achieved at the M.I.T. Lincoln Laboratory in the design, short-term stability[2] and long-term stabilization of $CO_2$ lasers. More recently, slightly modified versions of the same designs have been utilized in sealed-off CO laser experiments.[3,4] Also, these lasers have been successfully duplicated in a number of other laboratories with excellent results.

The lasers described in this paper were intended for applications in high resolution optical radar[5] and coherent detection at infrared wavelengths[6]. Therefore, short-term stability in a typical laboratory environment was of primary importance in the design of these lasers. Utmost coherence was desired for observation times ranging from about a millisecond to several seconds. The r.f. power spectral density of the signal obtained by heterodyning two lasers were utilized as a convenient and meaningful measure of stability.

Experiments leading to long-term stabilization of $CO_2$ lasers by utilizing the standing wave saturation resonance technique[7] originally suggested by A. Javan are also described; the preliminary results obtained in these measurements[8] may be improved by orders of magnitude with the use of more sophisticated experimental arrangements.

## II. LASER DESIGN

The short-term stability of single-frequency $CO_2$ lasers, together with the design and performance of earlier models of our stable lasers, have been previously described[2]. This paper will present hitherto unpublished details on our newer lasers, and some recent experiments performed with them.

Figure 1 shows the basic laser structure used during the last four years in our Laboratories. In order to achieve maximum open loop stability, a very rigid optical cavity, utilizing stable materials was chosen. Four thermally, magnetically, and acoustically shielded low expansion special invar alloy rods define the mirror spacing of the optical cavity. The mirrors are internal to the vacuum envelope, and are rigidly attached to the composite granite and stainless steel mirror holders bolted to the four invar rods. In spite of the rigid structure, the laser design is entirely modular, and can be rapidly disassembled and reassembled; mirrors may be rapidly interchanged, and mirror holders can be replaced by mirrors mounted on mechanical or piezoelectric tuners.

The relatively low voltage piezoelectric tuners have been designed to be usable within the vacuum envelope without causing voltage breakdown of the surrounding gas fill. Thus frequency tuning and modulation are accomplished while avoiding the problems experienced with the less stable Brewster-angle laser designs.

The direction of (the linear) polarization may be pre-selected by a grille within the optical cavity. The grille consists of three 2.5 micrometer diameter wires. Figure 2 is a photograph of a polarization selecting mode-limiting iris utilized on these lasers. The use of these wire polarizers

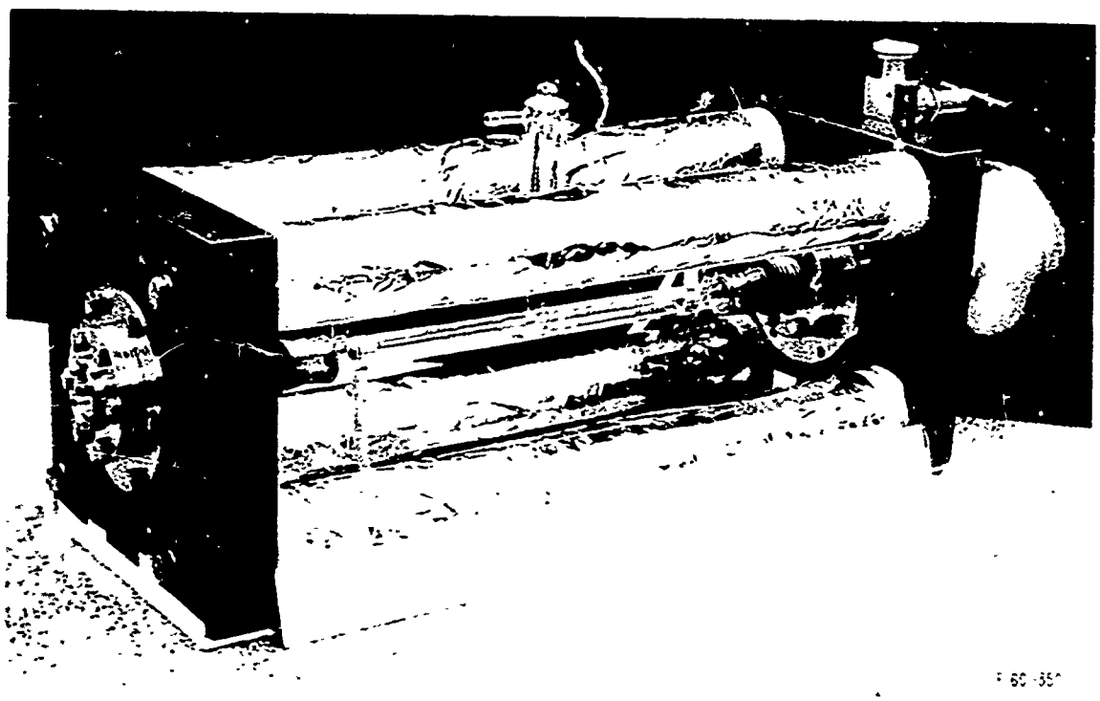

Fig. 1. 0.5 meter, internal mirror, piezoelectrically tuned stable $CO_2$ laser.

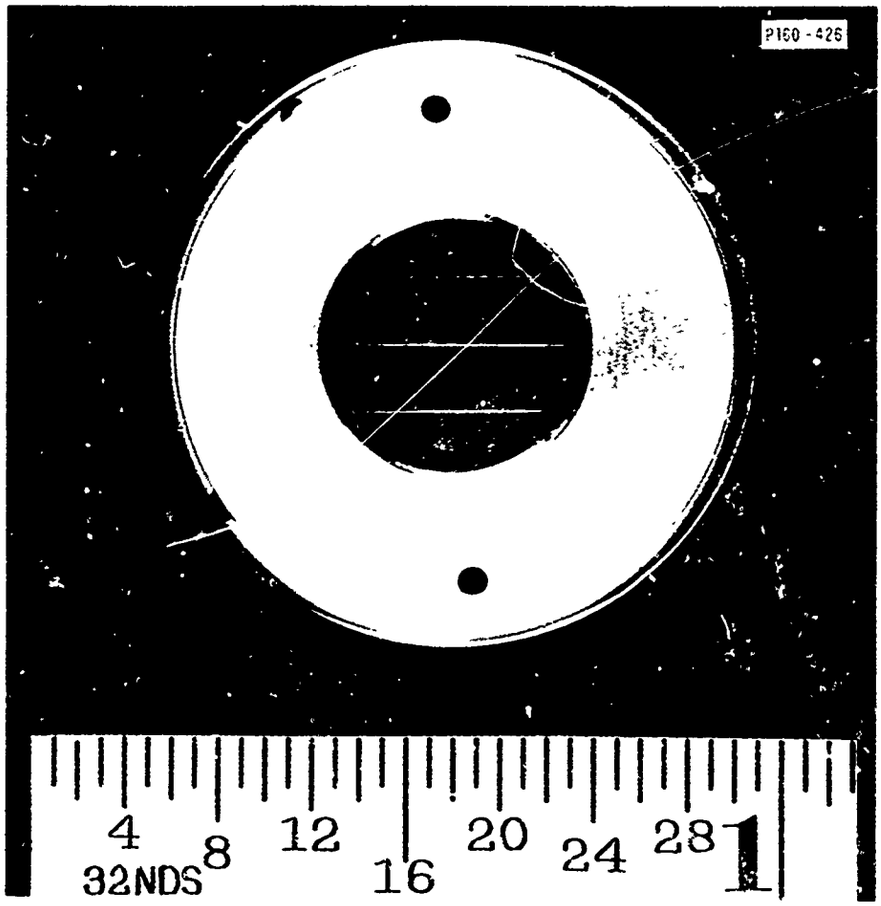


Fig. 2. Three-wire, polarization selector mode-limiting aperture.

has not resulted in any measurable decrease of power output and stability.

A number of grating-controlled lasers have been designed, constructed, and tested. In these lasers, a diffraction grating is substituted for one of the mirrors. This design feature enables the laser to operate in any preselected, single vibrational-rotational transition. Line competition is generally sufficient to produce single frequency output in the higher-gain $CO_2$ transitions even with a standard two mirror optical cavity. However, the use of frequency dispersive element(s) is necessary to insure single frequency operation in the low-gain $CO_2$ transitions. On the other hand, the cascade nature of the CO molecule's vibrational level structure, necessitates the use of frequency dispersive optical cavities at all times when single transition CO laser output is required.

Experimental evaluation of several of these grating-controlled lasers with a 150 cm semiconfocal cavity configuration have been performed. The output characteristics of these lasers were found to be highly reproducible both from one laser to another, and also as a function of time (over several months) in any one of the lasers tested to date. The resettability of the grating control mechanism exceeded all expectations. It was found that any one of the laser lines could be preset without the use of an auxiliary spectrometer, and the rms error in resettability was about 0.1 $cm^{-1}$. It should be noted that 0.1 $cm^{-1}$ corresponds to a grating position error of less than 5 arc seconds in the present design. Figure 3 is a photograph of a grating-controlled laser. These grating controlled lasers have been put to extensive use for the measurement of velocity cross relaxation rates among the vibrational-rotational levels of the $CO_2$ laser system[9].

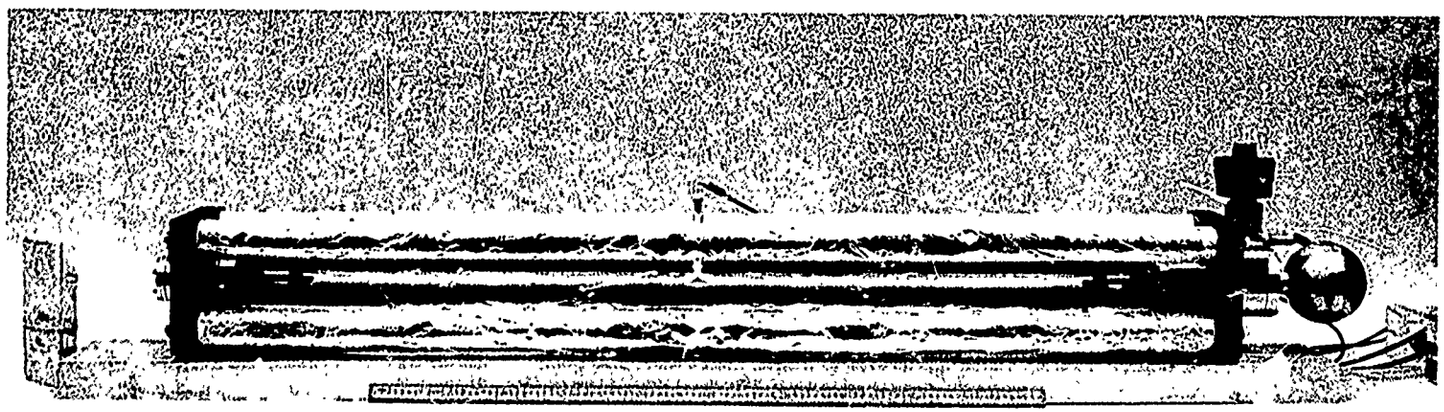

P160-537

Fig. 3. 1.5 meter, internal-grating-controlled, piezoelectrically tuned stable $CO_2$ laser.

More recently, grating-controlled lasers have been used almost exclusively in many CO laser experiments. The CO molecular system offers hundreds of lasing transitions from just below 5 microns to well above 8 micron wavelength. In our preliminary experiments, nearly two hundred individual vibrational-rotational transitions between 5 and 6.5 microns have been observed. A more systematic evaluation of sealed-off CO lasers is presently under way.

A variety of master and replica gratings were tested prior to their actual use in lasers. At least some of the grating families gave remarkably good and reproducible performance. About 94 ± 3% reflectivity into first order, very little loss and scattering, and grating-to-grating reproducibility (as a function of wavelength) within the tolerances of measuring equipment characterized the better diffraction gratings.

The modular nature of our laser design also allows the inclusion of gas absorption cells within the otherwise standard stable laser structure. Such absorption cells have been used to perform standing wave saturation resonance experiments[7] which in turn lead to the long-term frequency stabilization and to the measurement of pressure shift and pressure broadening in $CO_2$ lasers[8]. A more detailed description of the standing wave saturation resonance experiments will be given in another section of this paper.

## III. SHORT-TERM STABILITY MEASUREMENTS

Figure 4 shows the real time power spectrum of the beat signal between two free running lasers, similar to the one shown in Figure 1. The frequency scale of Figure 4 is 500 Hz/cm; this, of course, indicates that the optical frequencies of the two lasers producing the beat note was offset by less than $3 \times 10^3$ Hz. The discrete modulation sidebands are primarily due to line frequency harmonics, fan noise and slow drift; however, each spectral line is generally within the 10 Hz resolution bandwidth of the spectrum analyzer. The measurement of the spectral width was limited to 10 Hz resolution by the 0.1 sec observation time due to instrumentation and not by the laser stability itself. As a matter of fact, this picture was taken during normal working hours in a second floor room of our laboratory. A simple, fiberglass lined plywood box was used for the acoustic shielding of the lasers, and the entire experimental setup rested on a two ton granite slab floating on air mounts. Since the 10μm wavelength of $CO_2$ lasers corresponds to $3 \times 10^{13}$ Hz operating frequency, the 10 Hz linewidth indicates a frequency stability of better than 2 parts in $10^{13}$. The 10 Hz linewidth of Figure 4 implies among other things, that effective movements of the mirrors constituting the laser cavities had to be less than $10^{-3}$ Angstroms during the 100 millisecond observation time associated with the spectrum. Probably at least an order of magnitude improvement of the open loop frequency stability implied by Figure 4 could be obtained, if required, with the best presently available power supplies and without special modifications.

In most experiments, neither acoustic shielding nor shock mounting were used. Figure 5 shows a typical spectrum analyzer display of the beat signal of

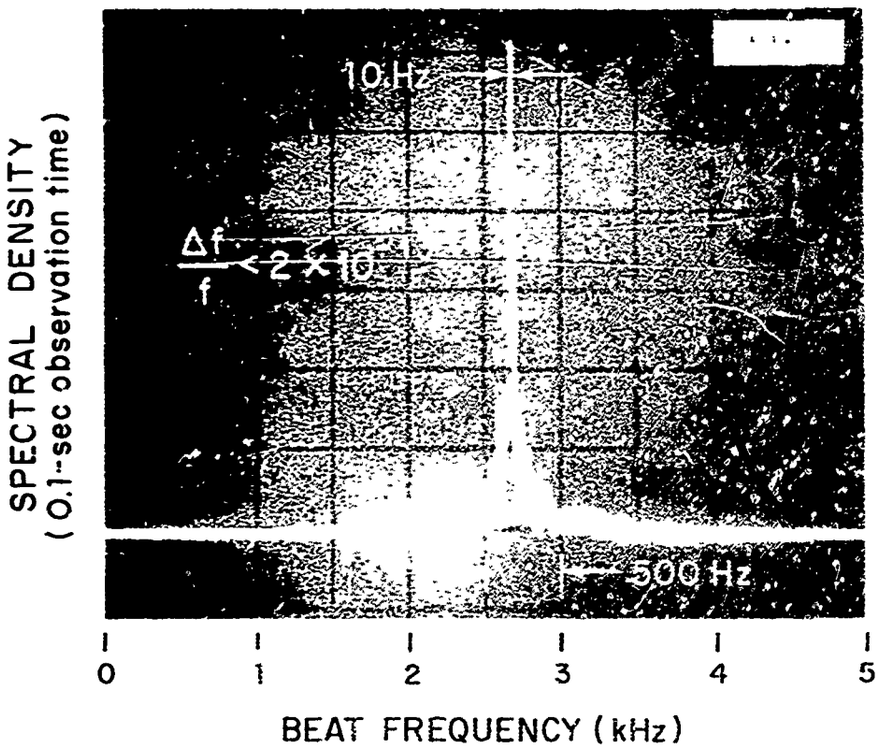


Fig. 4. Real-time spectral density of the beat signal of two free running, 0.5 meter stable $CO_2$ lasers for 0.1 second observation time; horizontal scale: 500 Hz/cm; Resolution 10 Hz.

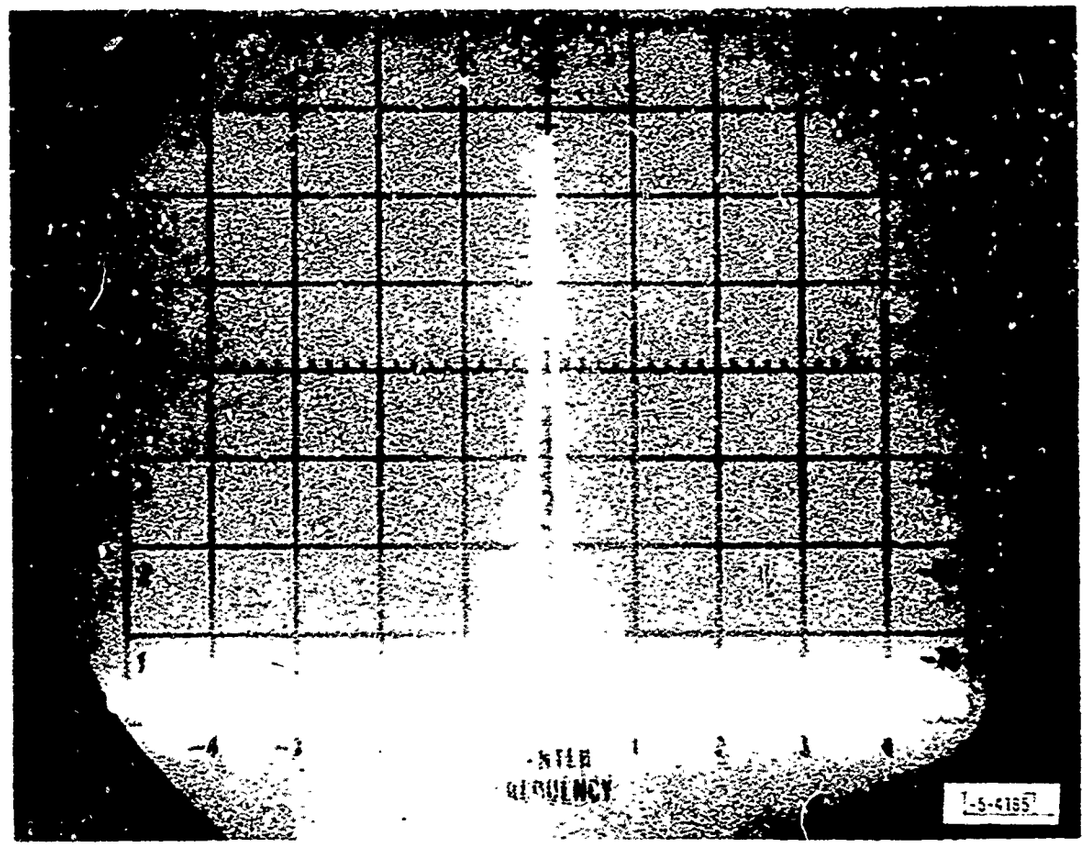

Fig. 5. Scanning spectrum analyzer display of the beat signal of a grating controlled laser and a standard 0.5 meter laser.

| | |
|---|---|
| Horizontal Scale | 50 kHz/cm |
| I.F. Bandwidth | 10 kHz |
| Scan Time | $5 \times 10^{-3}$ sec/cm |
| Film Exposure Time | 1/8 sec |

two lasers operating without any acoustic or vibration shielding. One of the lasers had a 15 watt grating-controlled output, and the power supplies used in obtaining Figure 5 exhibited more than two orders of magnitude larger peak-to-peak ripple than the ones used for Figure 4. Even though the frequency jitter displayed in Figure 5 was approximately $3 \times 10^3$ Hz, the frequency stability was more than adequate to obtain the resolution required for most experiments[9].

In spite of the excellent short-term stability of $CO_2$ lasers, the relatively broad gain profile of the inverted population (amplifying medium) allows laser operation to occur anywhere within an approximately 40 MHz frequency range centered around the oscillating transition. In many applications it is therefore desirable to find a narrow reference line within the operating frequency range of the laser, in order to compare and/or frequency lock the laser to this reference. Also, the short-term stability is optimum if the laser output is near the center frequency of the oscillating transition where the influence of external disturbances is minimum. Another problem may arise in $CO_2$ laser amplifiers driven by a stable oscillator because there may be significant differences in operating pressures along the master-oscillator amplifier chain. In this application, system performance may significantly depend on precise knowledge of both pressure broadening and pressure shift. Determination of pressure shift again requires some stable reference for comparison purposes.

The next section will present pressure shift and long-term stabilization experiments, which utilized the standing wave saturation resonance obtained with room temperature, low pressure, $CO_2$ absorption cells within the laser cavity.

## IV. STANDING WAVE SATURATION RESONANCE EXPERIMENTS

In a previous publication[17] some of the preliminary data on standing wave saturation resonance were reported. This paper will only briefly mention previously published results.

Figure 6 illustrates the standing wave saturation resonance experiment. Within a tunable, sealed-off, single frequency $CO_2$ laser oscillator indicated by the amplifying medium and the two cavity mirrors, we put an absorption cell which is separated by a Brewster-angle window from the active discharge.

In the experiment low pressure, room temperature $CO_2$ serving as the saturable absorber, is subjected to the standing-wave field of the laser cavity, with the laser oscillating in a single preselected transition anywhere between 9 and 11 microns. The saturation effect is detected by observing the change in the intensity of the entire collisionally coupled 4.3μ spontaneous emission band as the laser frequency is tuned across the Doppler profile of the corresponding 10μ absorption line. With a strong laser saturation field the intensity of the 4.3μ emission from the $CO_2$ absorber gas decreases resonantly by as much as about 25% of the total 4.3μ signal when the laser frequency $\nu$ is tuned within a frequency interval corresponding to the homogeneous width of the absorber and centered with the absorber's Doppler profile.

The alternate method of detection the standing wave saturation resonance of $CO_2$ directly in the 10μ output power of the laser, known as inverted Lamb dip, would yield a fractional change which is orders of magnitude smaller than the resonant change in the 4.3μ radiation. Thus, the measurement and utilization of the inverted Lamb dip resonance on the 10μ laser output requires

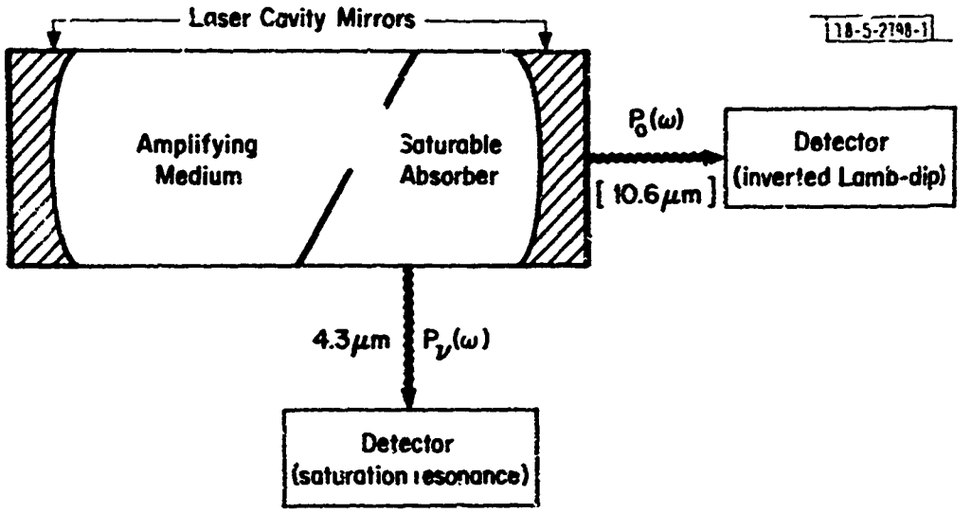


Fig. 6. Schematic principles of standing wave saturation resonance experiments.

a combination of relatively long absorption path, higher pressure and heating of the $CO_2$ absorber gas.

The relative weakness of the 10μ inverted Lamb dip saturation resonance is due to the very low absorption coefficient of room temperature $CO_2$ at 10μ wavelength; this may be explained by the energy level diagram of $CO_2$ shown in Figure 7. A particular preselected P or R branch oscillation corresponds to a transition between a single rotational level of the (001) upper vibrational state and another single rotational level of the (100) or (020) lower vibrational state. As Figure 7 shows, the lower state vibration-rotational levels of the $CO_2$ laser transition belong to a hot band and not the ground state. This explains the exceedingly low absorption coefficient of low pressure room temperature $CO_2$ at 10μ and the resulting difficulty in observing or utilizing the inverted Lamb dip resonance directly in the full power output of the $CO_2$ laser. In our experiments the saturation effect is detected by observing the change in the intensity of the 4.3μ spontaneous side emission over the entire (001) - (000) transition band as the laser frequency is tuned across the Doppler profile of the corresponding 10μ absorption line. The change in the entire band is due to the fact that a radiation-induced change in the population of an individual rotational level is accompanied by a change in the populations of all rotational levels of the same vibrational state; this is caused by the coupling among the rotational levels, which tends to maintain a thermal population distribution.

Figure 8 shows a close-up photograph of two lasers operating side by side. In the laser nearest to the foreground, the gas cell is visible to the right of the approximatley 20 cm long active discharge. A shielded,

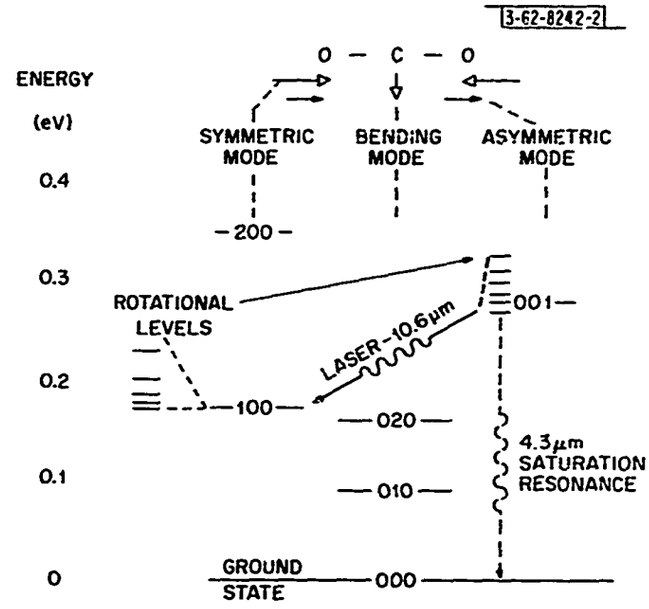


Fig. 7. $CO_2$ energy level diagram.

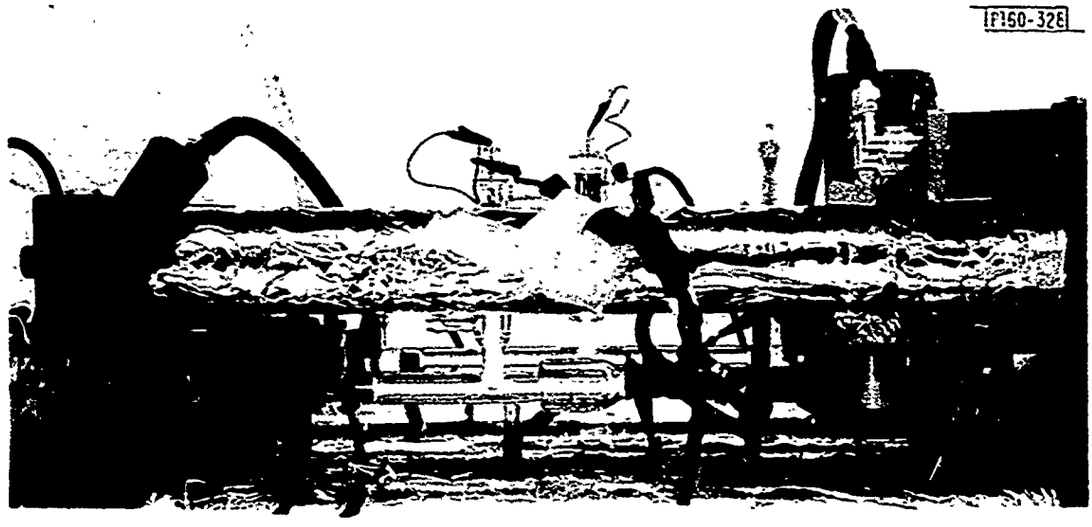


Fig. 8. 0.5 meter laser with internal absorption cell for standing wave saturation resonance experiments.

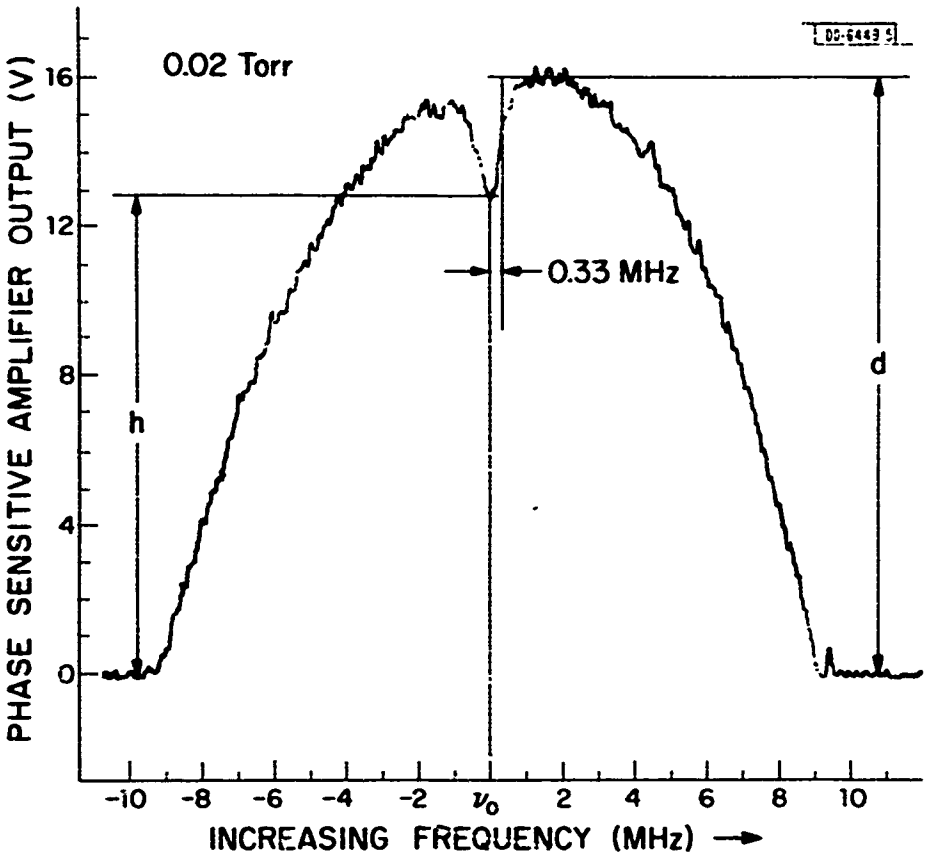


Fig. 9. 4.3μ signal resulting from the 10.59μ P(20) saturation laser transition as a function of laser tuning.

liquid nitrogen cooled indium antimonide detector measuring the 4.3μ spontaneous emission is also visible above the gas cell. In order to reduce the broadband background radiation, the detector is at the center of curvature of a gold coated spherical mirror which is internal to the gas absorption cell. Orders or magnitude increase both in signal and signal-to-noise ratio could be obtained with more sophisticated absorption cell and detector arrangements.

The total effective absorption path within the gas cell is approximately 3 cm. We have obtained systematic data for $CO_2$ pressures between .005 Torr and 0.8 Torr, with laser power outputs ranging from microwatts to a few hundred milliwatts.

In order to obtain accurate data, the second laser in the background of Figure 8 is operated at a fixed frequency and its output is heterodyned with the slowly tuned laser incorporating the absorption cell; the beat note of the two lasers in conjunction with a frequency discriminator is utilized to provide the frequency calibration of our experimental results.

Figure 9 shows a typical recorder tracing of the observed 4.3μ intensity change as the laser frequency is tuned across the 10.59μ P(20) line profile with 0.02 Torr pressure of $CO_2$ absorber gas. The standing wave saturation resonance appears in the form of a narrow resonant 20% "dip" in the 4.3μ signal intensity as the laser frequency is tuned acros. the center frequency of the absorbing transition's Doppler profile. The broad background curve is due to the laser power variations as the frequency is swept within its oscillation bandwidth. The peak laser power occurs at a frequency slightly shifted (about 0.33 MHz) from the center frequency of the corresponding low pressure absorbing line due to the pressure shift of the laser transition.

The laser was filled with 2 Torr $Co_2$, 2 Torr $N_2$, and 7 Torr He partial pressures. In order to better illustrate the pressure shift shown on Figure 9, we purposefully operated the laser at only about 0.5 milliwatt output power for this particular curve. At higher laser powers the 4.3μ signal response background curve would be much broader and the frequency shift of the resonant dip would not be as apparent to the eye. Figure 9 implies a pressure shift of less than 100 Hz/millitorr for the 10.59μ P(20) $CO_2$ transition; a very small pressure shift is of course desirable for clock applications. The pressure shift is determined more accurately by including two independent absorption cells within the optical cavity of a grating-controlled laser. Figure 10 is a photograph of such a twin-absorption cell assembly, prior to installation in the laser cavity. A separate detector-amplifier channel is used with each individual cell.

The pressure shift is measured by filling the two cells with the absorbing gases at different pressures. Figure 11 illustrates typical experimental data obtained by this technique. The absorption cells were filled to 0.03 and 0.280 Torr $CO_2$ gas pressure respectively, and the laser was tuned across the 9.55μ P(20) laser transition. The different widths of the two curves in Figure 11 clearly demonstrate pressure broadening; however, the rather small pressure shift in $CO_2$ cannot be easily measured from the relative displacement of such broad minima as exhibited by the two curves of Figure 11. To more accurately determine pressure shift, and also for frequency stabilization, it is convenient to obtain the derivative of the 4.3μ emission signal as a function of frequency. This 4.3 signal derivative may be readily obtained by modulating the laser frequency by a small amount as we slowly tune across

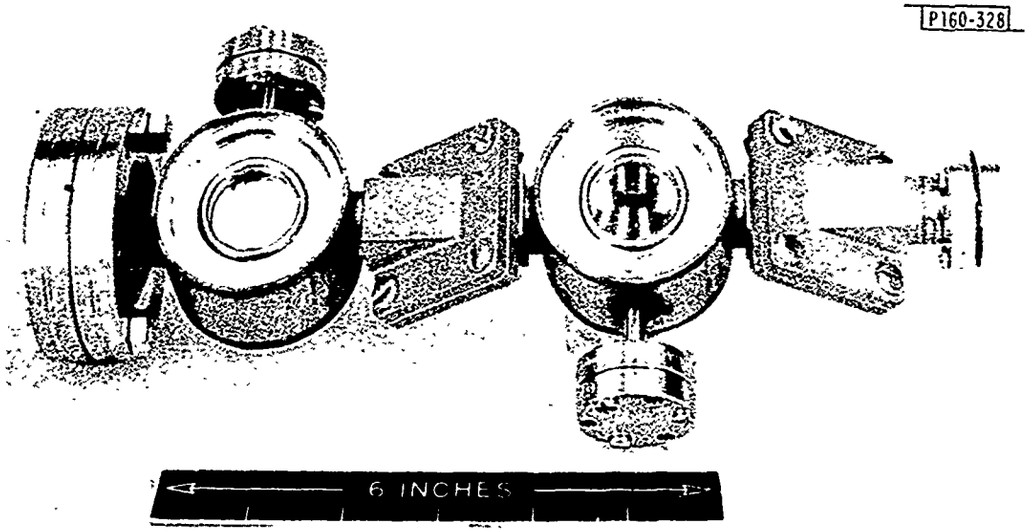


Fig. 10. Twin-absorption cell assembly before installation into the optical cavity of the laser.

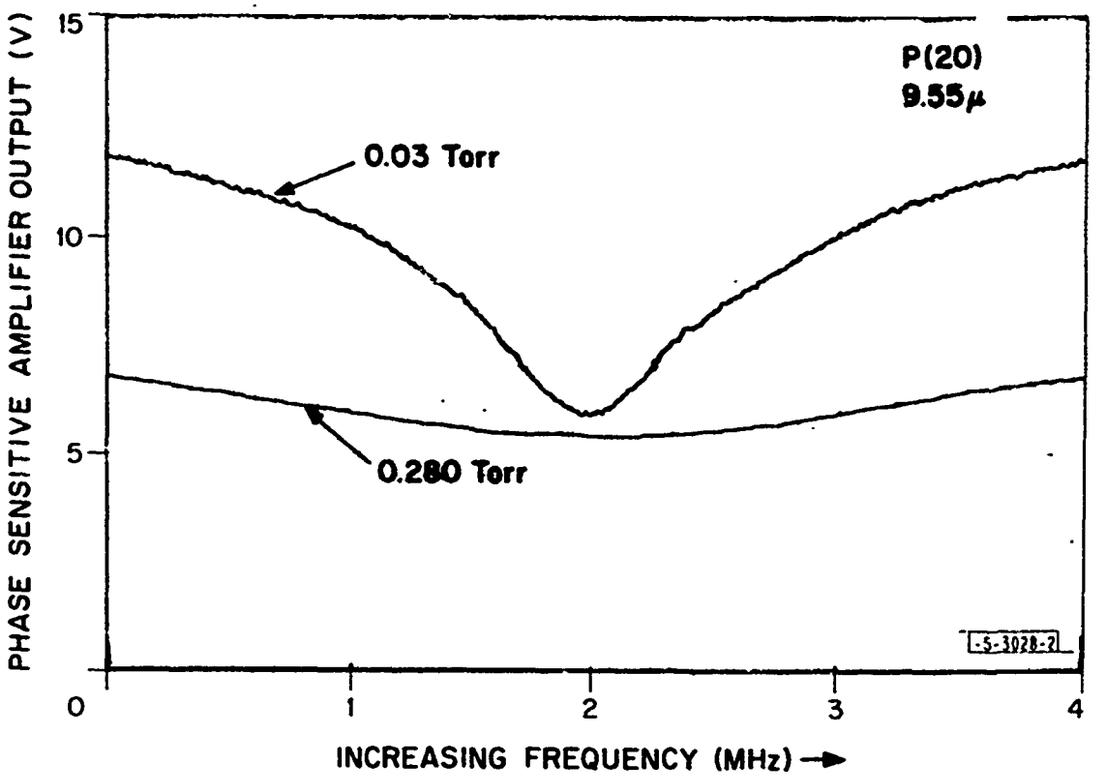


Fig. 11. 4.3μ signals resulting from the 9.55μ P(20) saturating laser transition as a function of laser tuning with two absorption cells within the laser cavity.

the resonance in the vicinity of the absorption line center frequencies. With the use of standard phase-sensitive detection techniques we can then obtain the 4.3μ signal derivative as demonstrated for instance by Figure 12; this figure shows the 4.3μ derivative signal as a function of laser tuning also near the center frequency of 9.55μ P(20) transition. In order to demonstrate resproducibility (by the similarity of the two 4.3μ derivative signals), identical, 0.05 Torr $CO_2$ pressure fill was used in both absorption cells to obtain Figure 12. Note that the parallel shift of the two curves is due to the intentional offset between the two recorder pens, and does not in any way signify pressure shift.

The 4.3μ signal derivative shown in Figure 13 illustrates its use as a frequency discriminator. The vertical scale is linear, with 0-voltage at the center corresponding to $\nu_o$ on the horizontal frequency scale. Any deviation from the center frequency $\nu_o$ yields a positive or negative phase detector output signal which may then be utilized in a feedback servo-loop. The approximately straight line running diagonally across Figure 13 is the frequency calibration signal obtained by heterodyning the 10.6μ output of one laser, slowly tuned across the absorption profile, with the 10.6μ output of the fixed frequency reference laser, as previously discussed. Figure 14 shows a block diagram of the experimental arrangement used in some of these measurements.

The width of the standing wave saturation resonance is usually dominated by collision broadening typically above 100 millitorr in our experiments[7]. In this relatively high pressure region the saturation resonance width is linearly proportional to pressure, and our measured results are in

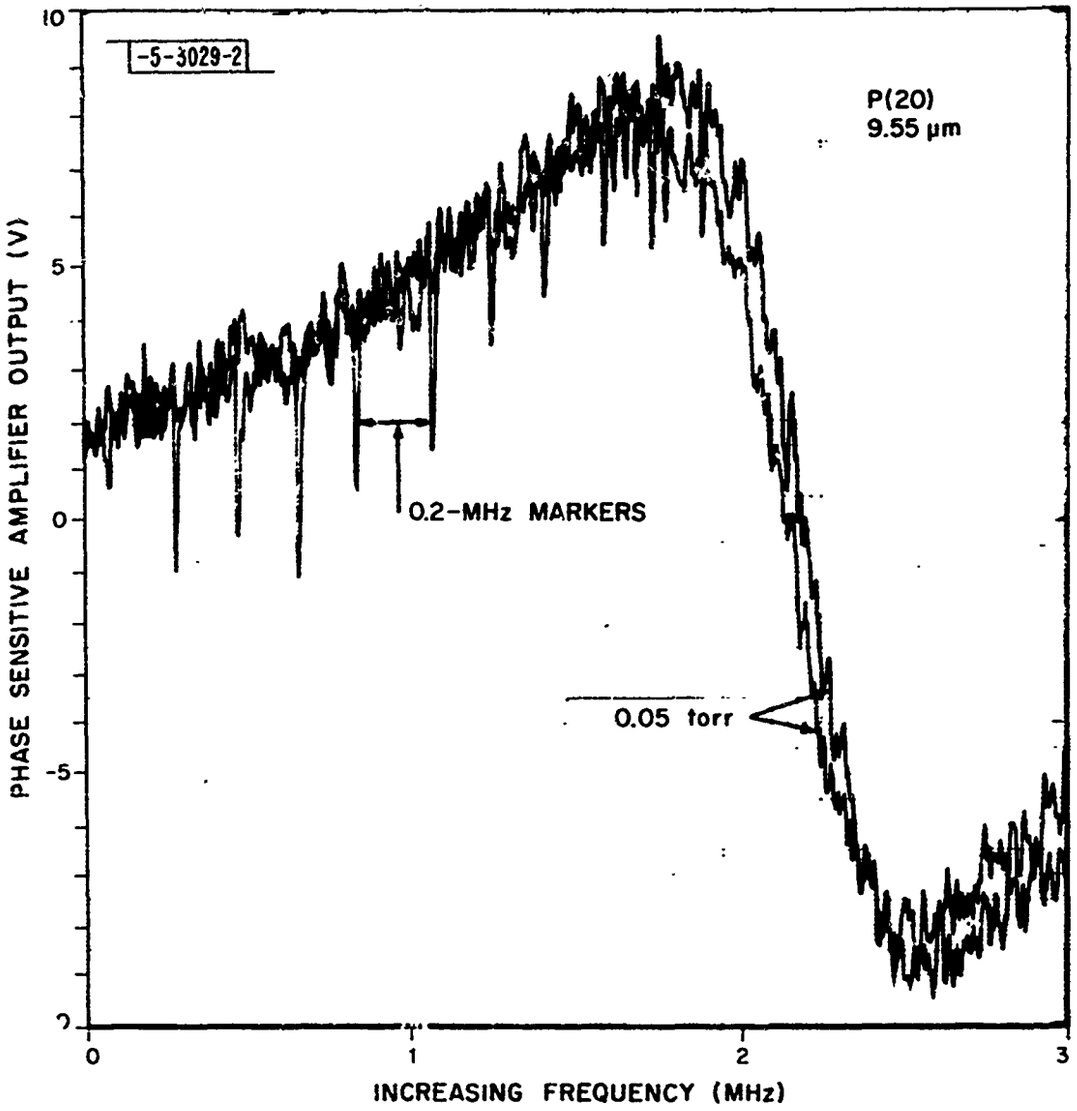


Fig. 12. 4.3μ derivative signals resulting from the 9.55μ P(20) saturating laser transition as a function of laser tuning with two absorption cells within the laser cavity.

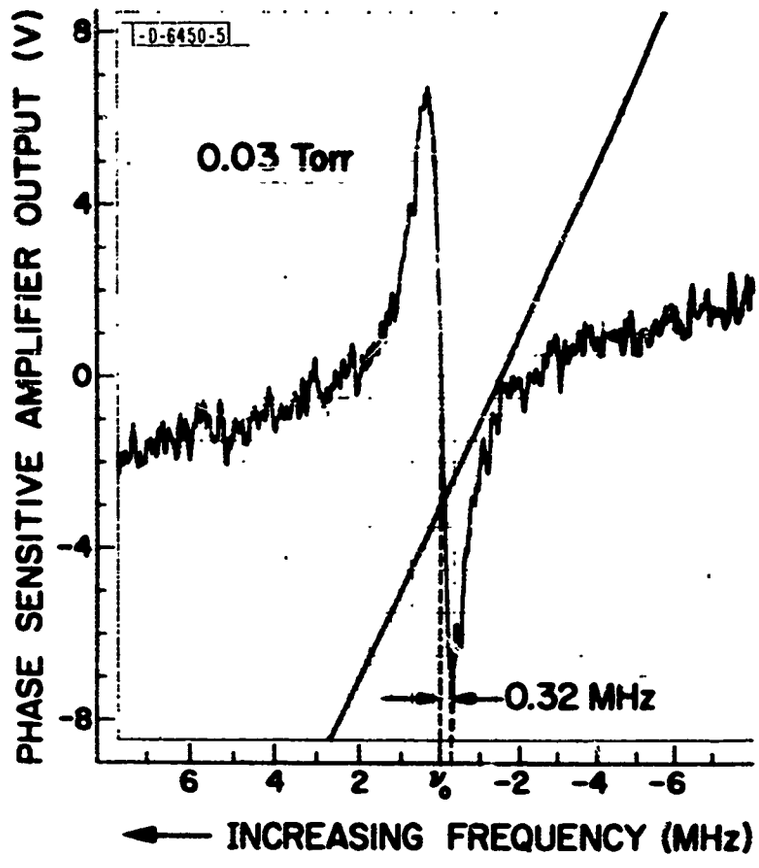


Fig. 13. 4.3μ derivative signal resulting from the 10.59μ P(20) saturating laser transition as a function of laser tuning.

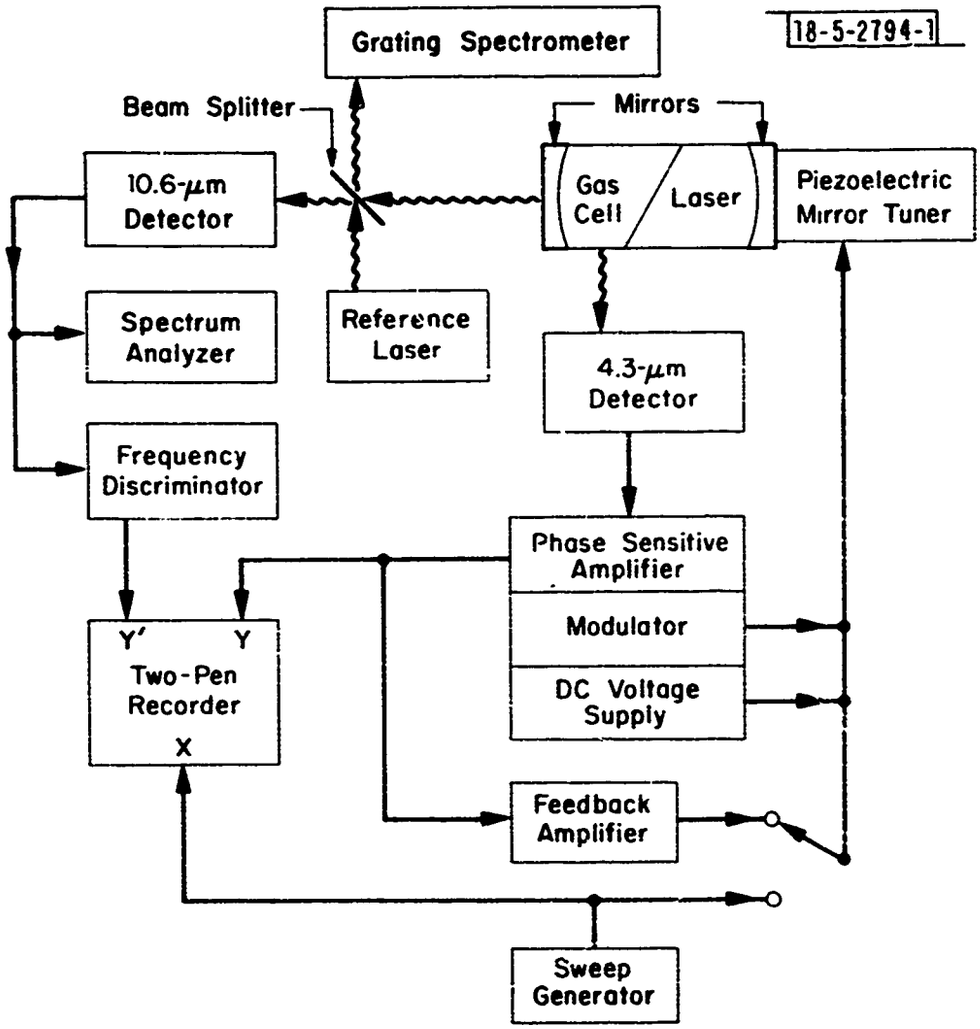


Fig. 14. Block diagram of experimental arrangement in standing wave saturation resonance experiments.

excellent agreement with the 7.6 MHz/Torr figure predicted by others from independent measurements of the absorption coefficient in relatively high pressure $CO_2$ gas cells[10]. For purposes of frequency reference and long-term stabilization, we are of course much more interested in the low pressure region of the resonance where the measured linewidths are narrow. In the limit of very low gas cell pressures, the linewidth is determined by power broadening and by the molecular transit time across the diameter of the incident beam. The two superimposed curves shown in Figure 15 clearly demonstrate the effect due to saturation of the absorption line. Laser power was the only parameter that was changed between the observation of the individual curves.

In these preliminary experiments half widths as low as 200 kHz have been observed. With the use of larger diameter laser beams, the limiting widths due to both power and transit time broadening can be considerably reduced.

We have utilized the frequency discriminator characteristics of the standing wave saturation resonances in conjunction with automatic feedback controls to stabilize the laser frequencies at the line profile centers of the various absorbing transitions.

Figure 16 shows a block diagram of our preliminary frequency stabilization experiment. Two of the lasers are independently locked to the $CO_2$ absorption profile centers. Each of the locked lasers is heterodyned with a third laser which is entirely free running. The resulting beat signals are fed to two discriminators, and the discriminator outputs are compared in a differential amplifier. By displaying the differential amplifier output and

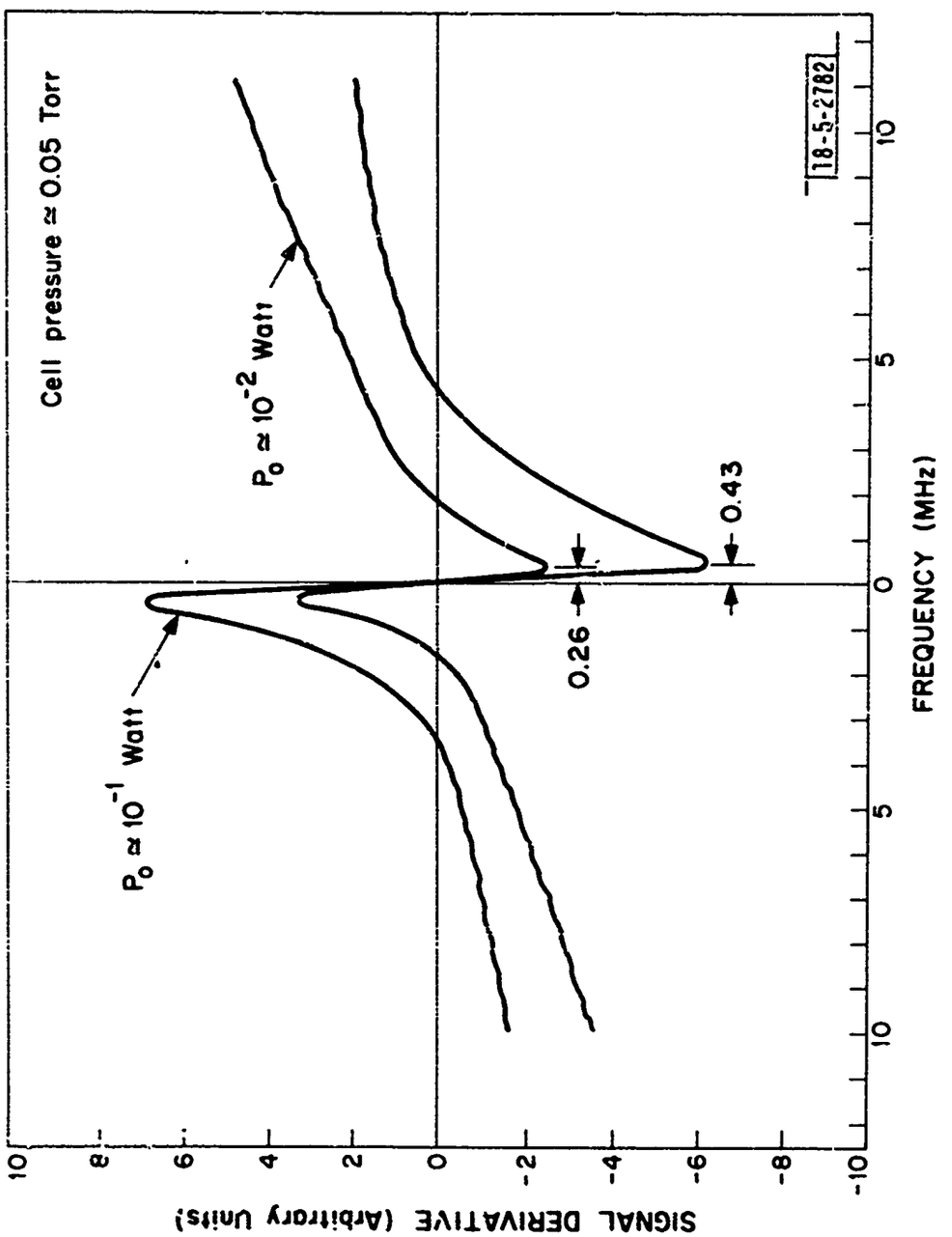


Fig. 15. Power broadening of the absorption line indicated by the increased line width for the higher saturating laser power output.

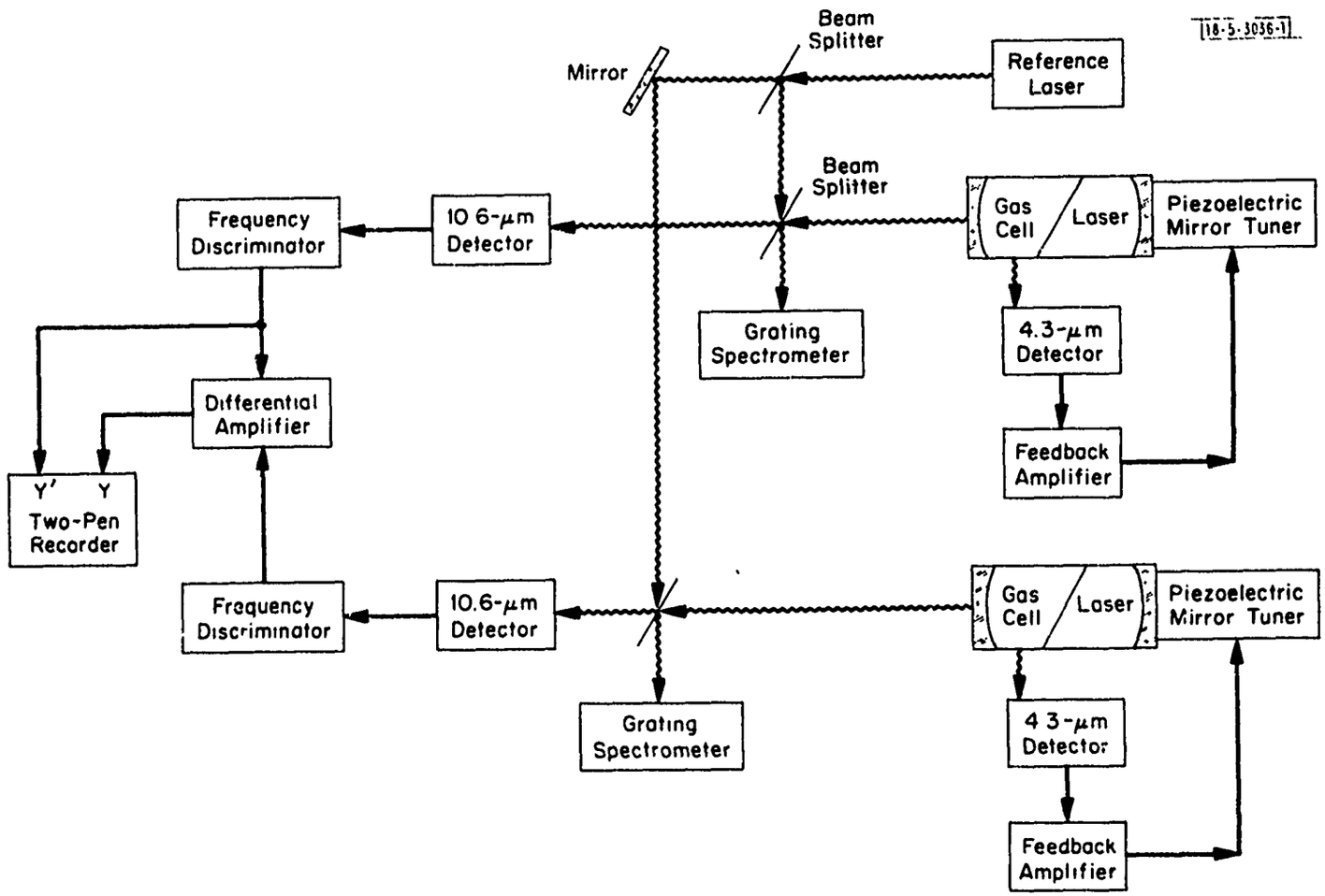


Fig. 16. Simplified block diagram of the closed-loop frequency stabilization experiment.

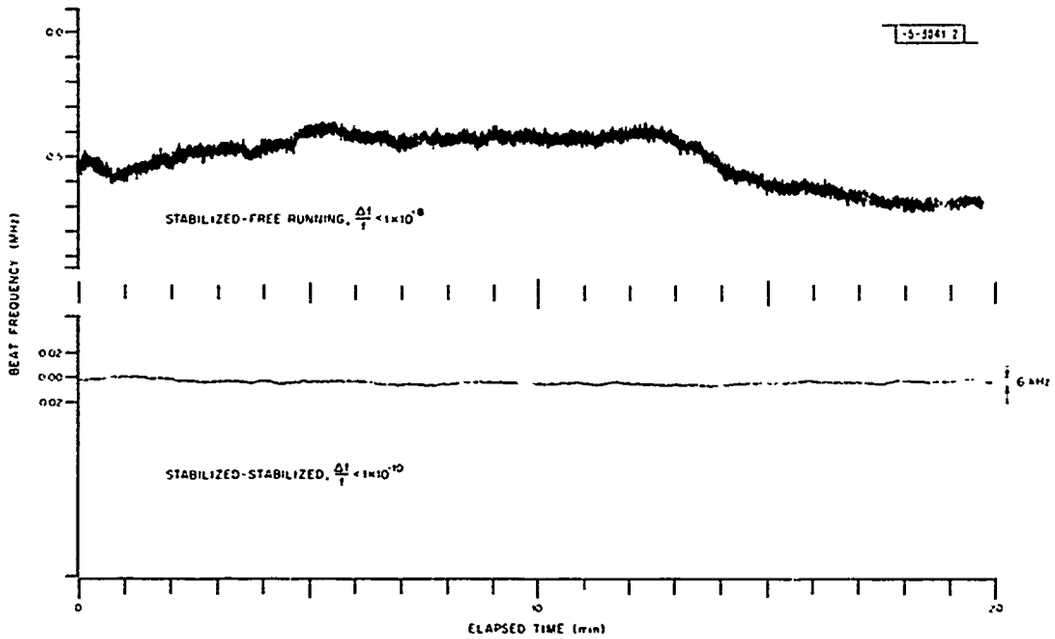


**Fig. 17. 20-minute segments of beat frequency recordings in the preliminary frequency stabilization experiment.**

one of the discriminator outputs on a two-pen chart recorder, we get a measure of long-term stability of both the free running and the stabilized lasers. Figure 17 illustrates a 20 minute segment of a recording which lasted several hours. The vertical scale of the upper trace is 100 kHz/cm, and such recordings indicate that 1 part in $10^{-8}$ open loop long-term stability can be achieved for many hours after some initial warm-up period.

The vertical scale of the lower trace has been expanded to 20 kHz/cm and, as the figure indicates, a long-term stability of 1 part in $10^{-10}$ has been achieved even with our first rather rudimentary closed-loop setup; very slowly responding power supplies and 30 second feedback time constants were used to obtain the result shown in Figure 17.

With the utilization of appropriately designed servo loops and with more sophisticated experimental arrangement at least two to three orders of magnitude improvement in long-term and even better short-term stability should be achieved.

## REFERENCES


1. C. Freed, "Design and Short-Term Stability of Single-Frequency $CO_2$ Lasers, IEEE J. Quan. Elect. QE-4, pp 404-408, June 1968.

2. C. Freed, "Advances in Stable $CO_2$ Laser Design and Performance", Paper 14.4 presented at the 1970 International Electron Devices Mtg., October 1970, Washington, D. C.

3. C. Freed, "Sealed-Off Operation of Stable CO Lasers", Appl. Phys. Lett. 18, pp 458-461, 15 May 1971.

4. C. Freed, "Sealed-Off Operation of Stable CO Lasers", Paper 4.7 presented at the 1971 IEEE/OSA Conference on Laser Engineering and Applications, June 1971, Washington, D. C.

5. T. J. Gilmartin, H. A. Bostick and L. J. Sullivan, "10.6μ $CO_2$ Laser Radar", NEREM Record, pp 168-196, 1970.

6. A rather interesting application of these lasers has been devised by a group under the guidance of C. H. Townes at the Univerity of California, Berkeley; M. A. Johnson constructed there two of the $CO_2$ lasers as part of a spatial interferometer for astronomical observations. The lasers are used as local oscillators in wideband (1 GHz) infrared heterodyne receivers. The intention is to put the receivers at the foci of two astronomical telescopes separated by as much as one kilometer. A portion of the output from one laser will be transmitted to the other; the resulting beat frequency will be used to phase-lock the lasers at a fixed offset frequency near 5 MHz. The radio-frequency outputs of the receivers will be brought together and correlated to yield information about the spatial intensity distribution of the observed source. The angular resolution will be .001 arc seconds for a one kilometer separation of the telescopes. This resolution is more than adequate to resolve the diameters of many stars and other interesting objects. Reproduction of the lasers created no serious problems; in fact, phase locking them proved to be easier than anticipated (M. A. Johnson, private communication).

7. C. Freed and A. Javan, "Standing-Wave Saturation Resonances in the 10.6μ Transitions Observed in a Low-Pressure Room-Temperature Absorber Gas", App. Phys. Lett. 17, pp 53-56, 15 July 1970.

8. C. Freed and A. Javan, "Standing-Wave Saturation Resonances in Room Temperature $CO_2$ 10.6μ Absorption Lines", Paper 4.4 presented at the 1970 Sixth International Quant. Elect. Conference, September 1970, Kyoto, Japan.

9. H. Granek, C. Freed, and H. A. Haus, "Experiment on Cross-Relaxation in $CO_2$", IEEE J. Quan. Elect. QE-8, pp 404-414, April 1972.

10. D. W. Ducsik and E. D. Hoag, "Determination of Collision Cross-Sections of $CO_2$, He, $N_2$, $O_2$, CO, $H_2O$ and the Radiative Lifetime of the (001-100) $CO_2$ Laser Transitions", Private communication.